Review

Cardiovascular MRI in childhood

Anil K Attili,[1] Victoria Parish,[2] Israel Valverde,[2] Gerald Greil,[2] Edward Baker,[2] Philipp Beerbaum[2]

[1]Departments of Radiology and Cardiology, University of Kentucky, Lexington, Kentucky, USA
[2]Evelina Childrens Hospital, Guys and St Thomas Foundation Trust, Division of Imaging Sciences, Kings College London, The Rayne Institute, London, UK

Correspondence to
Dr Philipp Beerbaum, Evelina Childrens Hospital, Guys and St Thomas Foundation Trust, Division of Imaging Sciences, Kings College London, The Rayne Institute, 4th Floor Lambeth Wing, Lambeth Palace Road, London SE1 7EH, UK;
philipp.beerbaum@kcl.ac.uk

Accepted 2 June 2010

INTRODUCTION

In recent years significant technical and clinical advances have resulted in the recognition of cardiovascular magnetic resonance (CMR) as a valuable tool for the comprehensive evaluation of diseases of the cardiovascular system in childhood. In contrast to echocardiography CMR is not limited by acoustic windows. It is non-invasive and avoids the use of ionising radiation and iodinated contrast when compared with invasive angiography. In current clinical practice, CMR is increasingly used in concert with other imaging modalities to provide high-resolution three-dimensional (3D) imaging of complex anatomy, accurate quantitative assessment of physiology and function and for tissue characterisation within the cardiovascular system. This review highlights the basic techniques and clinical applications of CMR in the evaluation of congenital and acquired diseases of the cardiovascular system in childhood.

CMR IMAGING TECHNIQUES
Background

The primary source of the signal used to construct MR images is derived from hydrogen protons (^{1}H). The highest concentration of ^{1}H protons are in water and fat. Through the use of a strong static magnetic field, much weaker but time-varying magnetic field gradients and short pulses of radiofrequency (RF) energy, the ^{1}H protons in selected regions of the body are stimulated to emit RF waves. These RF waves are then used to construct MR images. The strength of the static magnetic field in most clinical scanners used for CMR is 1.5 Tesla (T) (1 T =10 000 gauss (G); the strength of the earth's magnetic field at its surface is approximately 0.5 G). More recently MRI scanners with static field strength of 3 T have become available. An in-depth knowledge of underlying MRI physics enhances the quality of interpretation of the imaging data and is necessary for understandings its pitfalls and limitations. A detailed discussion of MRI physics is beyond the scope of this review and can be found in other sources.[1 2] A summary of cardiac MR techniques is provided below. The CMR examination should begin with a review of available prior clinical and surgical history and imaging data for each patient. The goal is to tailor the examination to the specific clinical questions posed by the referring physician, keeping scan times to a minimum. To realise its full potential and to avoid pitfalls CMR of paediatric heart disease requires training and expertise and is best undertaken by specialists working in close collaboration with paediatric cardiologists and surgeons managing the patients.

## Motion compensation during cardiac MRI: cardiac and respiratory gating

Cardiac and respiratory motion during MR image acquisition results in image blurring. Therefore, strategies for motion compensation are mandatory to achieve good image quality. The most common approach to compensate for cardiac motion is to synchronise image acquisition with the cardiac cycle using either prospective or retrospective electrocardiographic gating.[2] Accurate R-peak detection is critical for good-quality scans. Most MR systems currently use advanced triggering modules based on vectorcardiography to improve R-wave detection in the MR environment.[3] Blurring due to respiratory motion is most commonly avoided by acquiring the images during a breath hold usually in end expiration. In patients who are unable to breath hold, it is usually possible to obtain diagnostic quality cine images by averaging out respiratory motion artefact with the use of multiple signal averages during free breathing.[2] An alternative approach to respiratory motion compensation during free breathing acquisitions is to detect and synchronise acquisition to respiratory motion using an external respiratory sensor (bellows). More recently, navigator echo respiratory gating techniques have been developed to accurately and reproducibly monitor and correct for respiratory motion of the heart.[2] The navigator echo method uses an MR signal to detect and monitor diaphragm position during a free breathing image acquisition. The primary applications for navigator gating are high-resolution 3D isotropic imaging for intracardiac anatomy and MR coronary angiography. Another approach to respiratory and cardiac motion compensation is to use real-time MR imaging as the effects of cardiorespiratory motion on image quality become less pronounced at a frame rate of >15–20 images per second. Hence, real-time imaging can be performed during free breathing and without cardiac gating; however the benefit comes at the cost of a lower spatial and temporal resolution. Despite these drawbacks real-time imaging has still shown to be accurate for the quantification of left-to-right shunts in children[4] and for the measurement of left ventricular systolic function as compared with breath hold MRI.[5]

Overview of sequences used in cardiovascular MRI

The building blocks of an MRI examination are called pulse sequences. An MRI pulse sequence describes the way in which the magnetic field gradients and RF gradients are applied to produce images with particular characteristics. Two classes
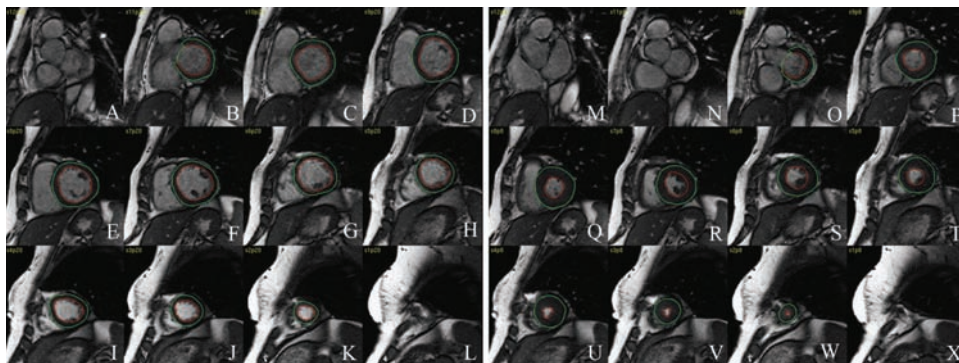
Figure 1 Evaluation of left ventricular function by CMR. Short axis views of the entire left ventricle from base to apex in diastole (A-L) and systole (M-X). Delineation of the epicardial and endocardial contours allows calculation of left ventricular mass, end diastolic volume, end systolic volume, stroke volume and ejection fraction.
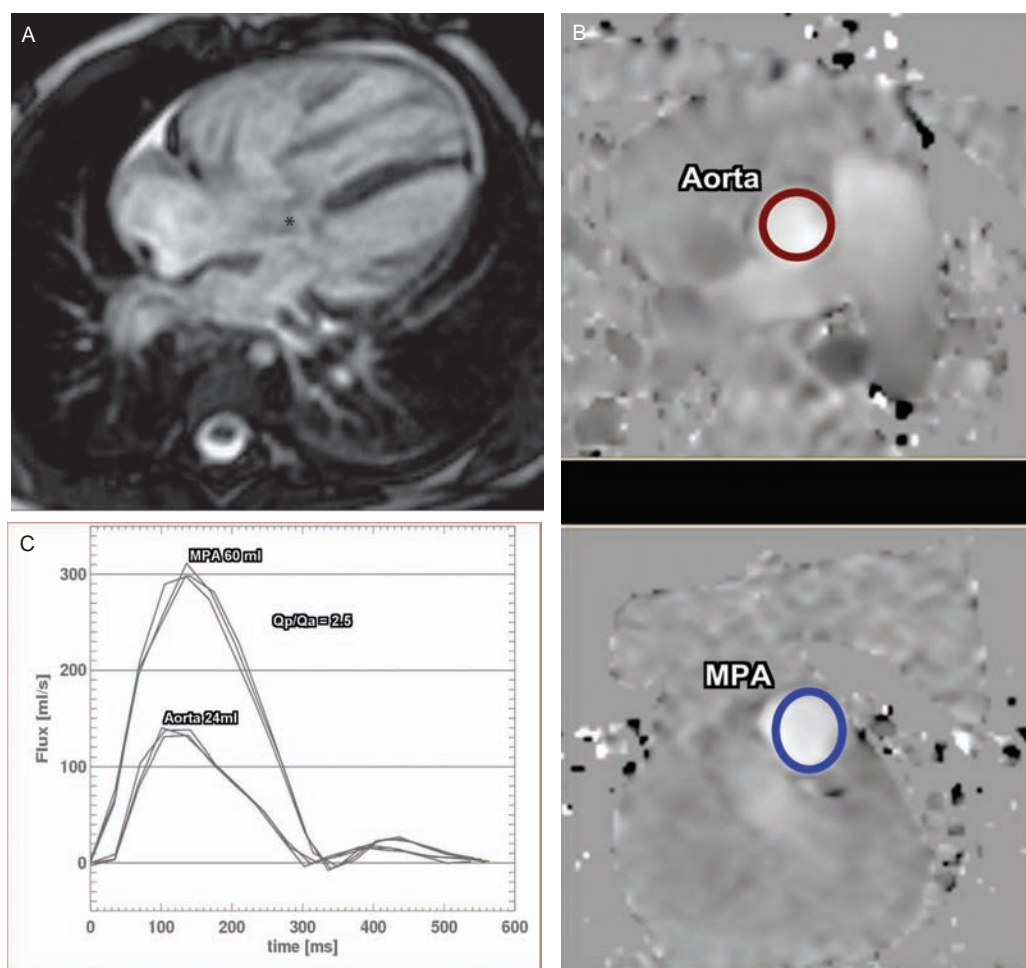

Figure 2 Atrioventricular septal defect (AVSD). (A) Horizontal long axis view of the heart using a bright blood sequence shows the defect (asterisk). (B) Phase contrast imaging through the aortic root and the main pulmonary artery. The circles are regions of interest drawn to calculate flow within the vessels. (C) The calculation of the left to right shunt by estimating the Qp/Qa is shown.

of pulse sequences used in MR are spin-echo (black blood) and gradient-echo (bright blood) sequences.
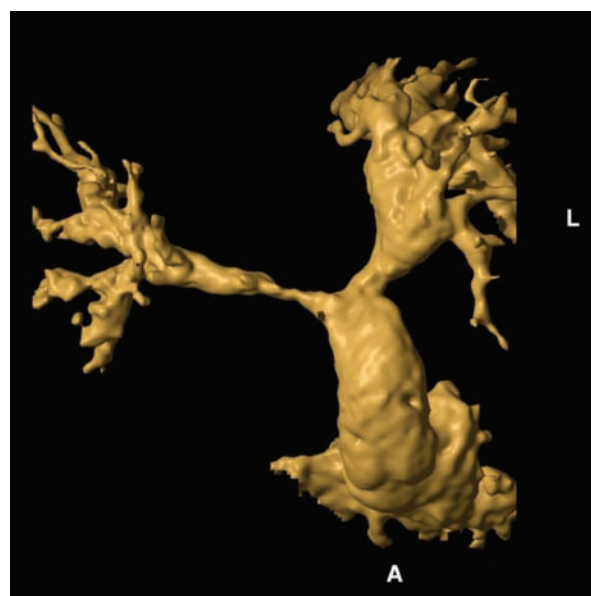
Spin-echo sequences
On spin-echo sequences blood vessel lumina appear black when flowing spins move out of the image plane between excitation and signal read-out. The addition of a preceding inversion recovery preparing pulse pair to a spin-echo sequence further suppresses the signal from flowing blood in the ventricles and large vessels to produce black-blood sequences with enhanced image quality.[6] Black-blood sequences provide excellent anatomic detail of cardiac chambers, great vessels and pericardium and are relatively unaffected by metallic artefact. A unique feature of MR is
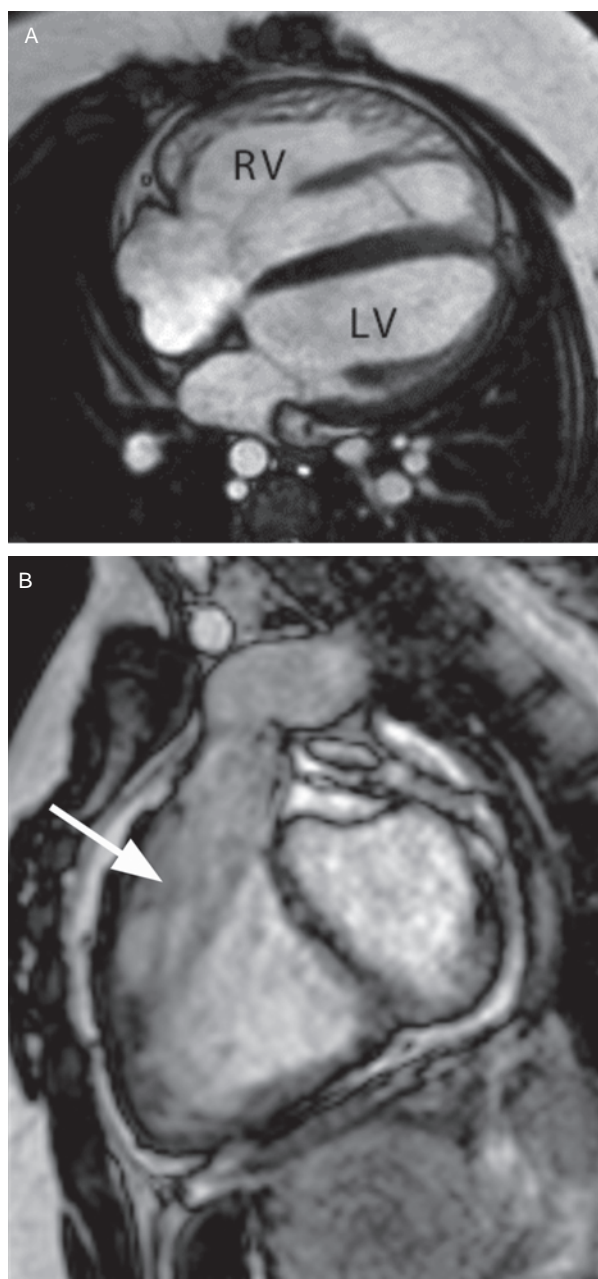
Figure 3 Status post TOF repair. (A) Markedly dilated right ventricle seen on a horizontal long axis (4 chamber) view. (B) Right ventricular outflow tract view in diastole shows severe pulmonary regurgitation (the regurgitant stream flowing back into the right ventricle is arrowed). Phase contrast imaging estimated the regurgitant fraction to be 70% (not shown).

Figure 4 Bilateral pulmonary artery stenosis post repair of TOF as shown on a volume rendered reconstruction from a 3D Gadolinium enhanced MRA.

its superior contrast resolution in comparison to other cross-sectional imaging modalities. Image contrast in MR is created by differences in the strength of the signal recovered from different locations within the sample. This depends upon the relative density of excited nuclei (usually water protons), on differences in relaxation times of those nuclei after the pulse sequence, and often on other user-defined parameters. The parameters of a black-blood imaging sequence can be adjusted to enhance or suppress certain tissue, for example, fat and inflammatory tissue. Commonly used sequences for tissue characterisation include T1- and T2-weighted sequences based on the differences in

longitudinal and transverse relaxation times of protons in tissues following an RF pulse application. Tissue characterisation by MR is further described in the section of cardiac masses below.

Gradient-echo sequences
Gradient-echo sequences have increasingly become the mainstay of cardiac MRI as they allow dynamic imaging of cardiac and vascular anatomy. Gradient-echo sequences have fairly low soft-tissue contrast compared with spin-echo sequences, and flowing blood is represented by high signal intensity and turbulence as areas of signal void. Gradient-echo sequences are used in assessment of valvular lesions, shunts, great vessels, and in the evaluation of ventricular function and wall-motion characteristics. Fast acquisition enables multiple phases of the cardiac cycle to be acquired, which can be reconstructed into a cine loop format that allows visualisation of cardiac motion and blood flow. The current standard gradient-echo sequence used in cardiac MR is known as the cine steady state free precession (SSFP) sequence, which permits more reliable distinction of the endomyocardial border, less sensitivity to slow flow and a relatively faster acquisition time as compared with earlier techniques.[7] [8] Multi-slice 'stacked' 2D cine SSFP imaging is the best available in vivo test for ventricular volumetry, as it is not reliant on geometric assumptions (figure 1). Multiple studies have demonstrated that measurements of ventricular dimensions and function by CMR are highly accurate and reproducible.[9–11] Recently 3D SSFP techniques have been developed that allow near isotropic imaging of the entire cardiac volume. This technique allows accurate multiplanar reformatting of any desired image plane during postprocessing and is particularly useful for the assessment of complex congenital heart disease (CHD)[12] including coronary artery anatomy.[13] An important capability of MRI is the quantification of blood flow and velocity. Gradient-echo techniques can be phase-encoded so that information regarding blood flow and velocity can be acquired. The technique known as
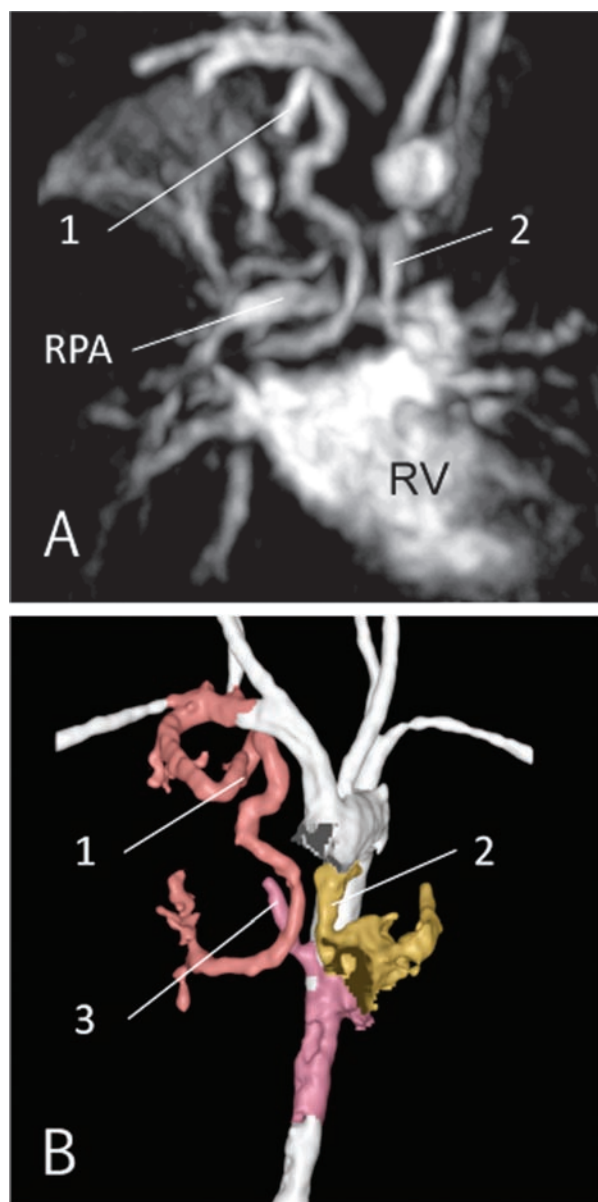
Figure 5 Major aortopulmonary collateral arteries (MAPCA) in a 10-month-old boy with TOF and pulmonary atresia as shown on Gadolinium enhanced MRA. (A) Contrast enhanced picture, anterior view. Right ventricle (RV) and right pulmonary artery (RPA). From the right subclavian artery, there is a first MAPCA (1) to the right lung which is very tortuous and travels down to reach the upper right pulmonary lobe. There seems to be a connection to the RPA distally. Below the aortic arch, there is a second MAPCA (2) to the left lung. (B) 3D shaded volume reconstruction anterior view. The RV and RPA have been removed to show a third MAPCA (3). It origins after the left subclavian artery origin and travels to the right lung, ascending towards the upper right pulmonary lobe.

velocity-encoded phase-contrast MR is used for the quantification of pulmonary to systemic blood flow[14] (figure 2), valvular regurgitation[15] and vascular stenosis[16] in order to assess disease progression, suitability and timing for surgery. In vivo and in vitro studies have shown that the measurement of blood flow by velocity-encoded MR is accurate and reproducible.[14 17]

The administration of intravenous MR contrast agents based on gadolinium chelates allows the performance of 3D contrast-enhanced MR angiography (3D CE-MRA) providing high spatial and contrast resolution data useful in delineating thoracic vascular anatomy. More recently, time-resolved 3D MRA has been developed and vailated to appreciate for example dynamic changes of pulmonary perfusion.[18] Postprocessing algorithms including surface and volume rendering and curved multiplanar reformation of the raw data acquired by 3D CE-MRA help to delineate and better understand complex vascular anatomy. Other advanced MR gradient echo sequences are used in the assessment of myocardial perfusion, viability and strain imaging (tagging).

SAFETY ISSUES AND SPECIAL CONSIDERATIONS IN CHILDREN

CMR is safe provided adequate precautions and guidelines to prevent potential adverse events are taken into consideration.[19 20] Potential hazards in MRI result from the effects of the static magnetic field, RF energy and time-varying magnetic field gradients used for image creation. Short-term exposure to the static magnetic fields used for medical imaging has not been shown to cause adverse biological effects. Risks of exposure to static magnetic fields are primarily related to implanted or foreign metallic objects and external ferromagnetic objects that may become projectile near the magnet. Patients and accompanying relatives must be carefully screened for metallic objects or metal devices before entering the MRI suite. Most implants used in patients with heart disease for example sternal wires, heart valves, stents, occluding devices and coils are not considered contraindications to MRI, although an image artefact local to the implant may be present. Care is required in patients with cerebrovascular clips and cochlear implants however, and specialist advice is needed for such patients.[19] The RF pulses used in MR imaging result in power deposition in human subjects that is transformed into heat. The measurement used to describe the absorption of RF energy is the specific absorption rate (SAR). SAR limits are incorporated in the design of commercial MR pulse sequences to ensure that maximum changes in tissue temperature are kept below regulatory guidelines.[21] Hazards associated with RF fields are typically related to exposed wires, electrical cables or loops of conductors in which current is generated, potentially causing burns. Therefore exposed, crossed or looped wires, direct contact between the subject's skin and RF transmit coils and skin-to-skin contact points that create closed loops must be strictly avoided. The rapid switching of magnetic field gradients used in certain types of pulse sequences can result in peripheral nerve stimulation. However, this risk is minimised by safety standards limiting the maximum rate of rise of magnetic field gradients.[21] Pacemakers and implanted cardioverter defibrillators are considered strong relative contraindications to MR although some reports of success do exist, and there is progress towards manufacture of CMR-compatible devices.[22]

Nephrogenic systemic fibrosis is a potentially fatal multisystem fibrosing disorder primarily affecting the skin and has been strongly associated with the use of gadolinium-based contrast agents in patients with severe renal impairment (glomerular filtration rate <30 ml/min/1.73 m^2). The use of gadolinium-based contrast agents for CE-MRA must be avoided in these patients.[20]

Children under 8 years of age cannot cooperate with a typical CMR examination and the use of deep sedation or general anaesthesia performed by anaesthesiologists specialising in paediatric cardiac care is preferred. Cardiac MRI can be
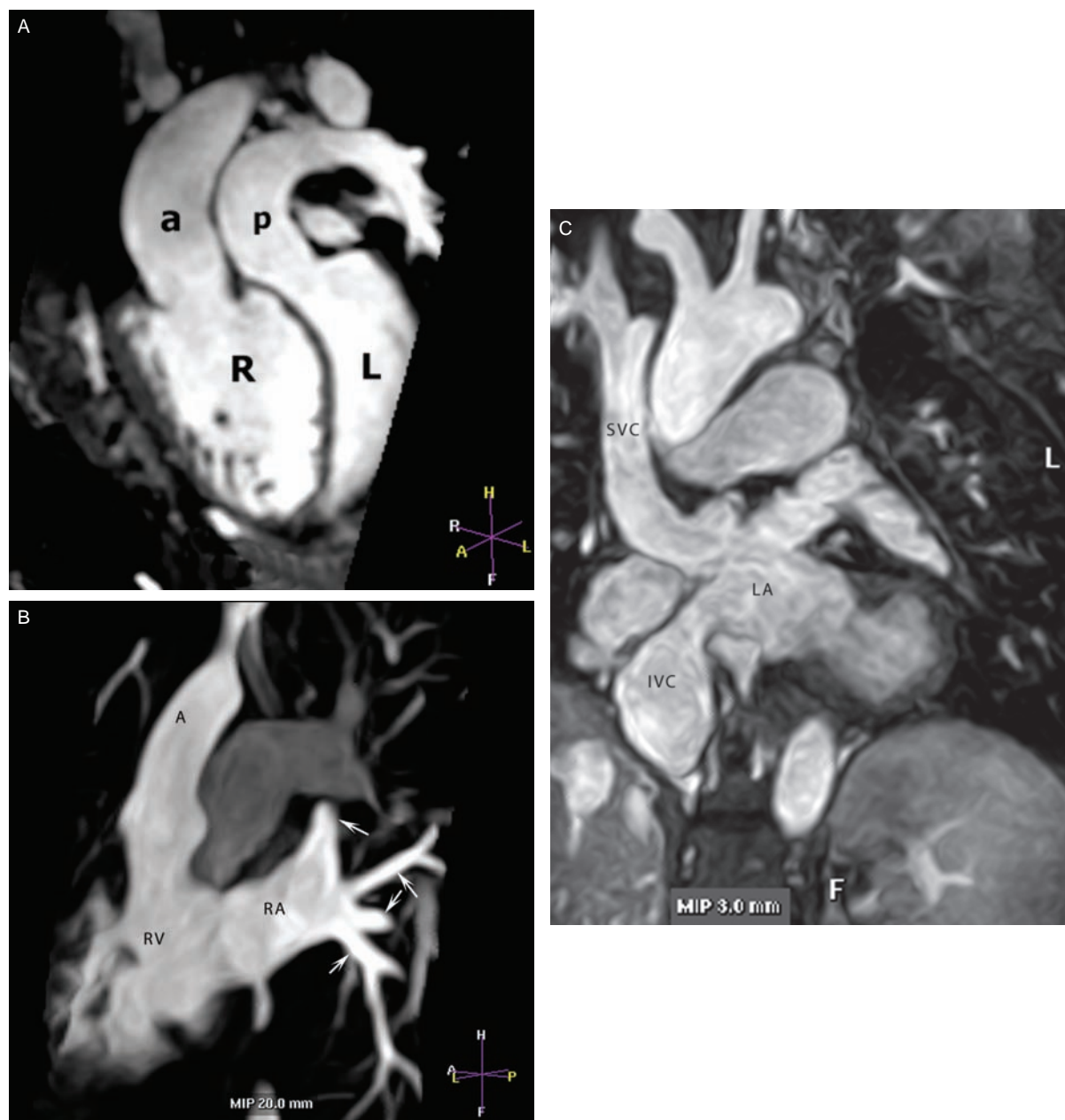
Figure 6 D-TGA post atrial level switch (Mustard procedure). (A) Oblique coronal reconstruction from a 3d-SSFP acquisition showing the aorta (a) arising from the right ventricle (R) and the pulmonary artery (p) arising from the left ventricle (L). (B) Oblique sagittal maximum intensity projection from a gadolinium enhanced MRA shows the pulmonary veins (arrows) being directed to the right atrium with baffles which are patent without stenosis. (C) Oblique coronal maximum intensity projection from a gadolinium enhanced MRA showing the SVC and IVC baffles directing blood into the left atrium. The baffles are patent without stenosis.

safely performed with low risk even in critically ill infants referred from a paediatric cardiac intensive care unit, however it requires great care and multidisciplinary expertise.[23] Some patients over 8 years are capable of cooperation, whereas most children over 10 years are capable of undergoing a CMR examination without general anaesthesia or sedation provided their mental development is age appropriate and they are not claustrophobic.

CLINICAL APPLICATIONS – CHD

CMR is an important diagnostic tool for CHD, as reflected by class 1 recommendations for its use by various consensus panels.[24 25] In this group of patients CMR provides clinically relevant information and is usually appropriate; it may be

used as a first-line imaging technique and is supported by substantial literature. A significant strength of CMR is the ability to obtain 3D contiguous data sets which are very effective for the complete depiction of the pathological anatomy of both simple and complex CHD. The sequential monitoring of ventricular dimensions and function is important during follow-up. CMR provides more precise and reproducible quantification of ventricular volumes, mass and function than 2D echocardiography.[25] This is especially the case for the right ventricle, which is usually the chamber implicated in and stressed by repair of CHD.[26 27] The lack of ionising radiation is an important consideration when performing sequential studies in children and young. However, the clinical use of CMR depends on the age and the clinical condition of the

patient. General anaesthesia is required in small children and monitoring is demanding in critically ill infants.[23] Thus, CMR is usually performed following, and as an adjunct to, transthoracic echocardiography in neonates and infants. In contrast, CMR becomes the first-line technique when in older children, in adolescents or adults, in more complex anatomy or at any age after surgery because body habitus and interposition of

scar tissue and lungs become an increasing problem for transthoracic echocardiography. The need for and duration and risks of diagnostic catheterisation can be minimised by prior use of CMR.

CMR protocols in the imaging of CHD

A number of generally applicable protocols have been suggested for a thorough investigation of a patient with CHD (table 1).[28] These protocols may be modified to address a particular clinical question.

Role of CMR in major specific congenital heart defects
#### Tetralogy of Fallot

Tetralogy of Fallot (TOF) is the most common form of cyanotic CHD and accounts for approximately 10% of all CHD. The main role of MRI in patients with TOF is in the assessment of postoperative complications. Operative repair of TOF consists of resection of the infundibular stenosis, enlargement of the pulmonary valve/annulus and closure of the VSD. The most common late postoperative complication is pulmonary regurgitation leading to progressive right ventricular dilatation and dysfunction (figure 3). In addition patients with repaired TOF may have branch pulmonary artery stenosis (figure 4) and residual aortopulmonary collaterals. MRI is indicated in these patients to quantify the degree of pulmonary regurgitation, identify the location and severity of pulmonary stenosis and quantify right and left ventricular volumes and function. This unique information provided by CMR has prognostic and therapeutic implications for the management of these patients.[29] [30] CMR assessment in conjunction with clinical and electrophysiological data is used to direct further care in patients with repaired
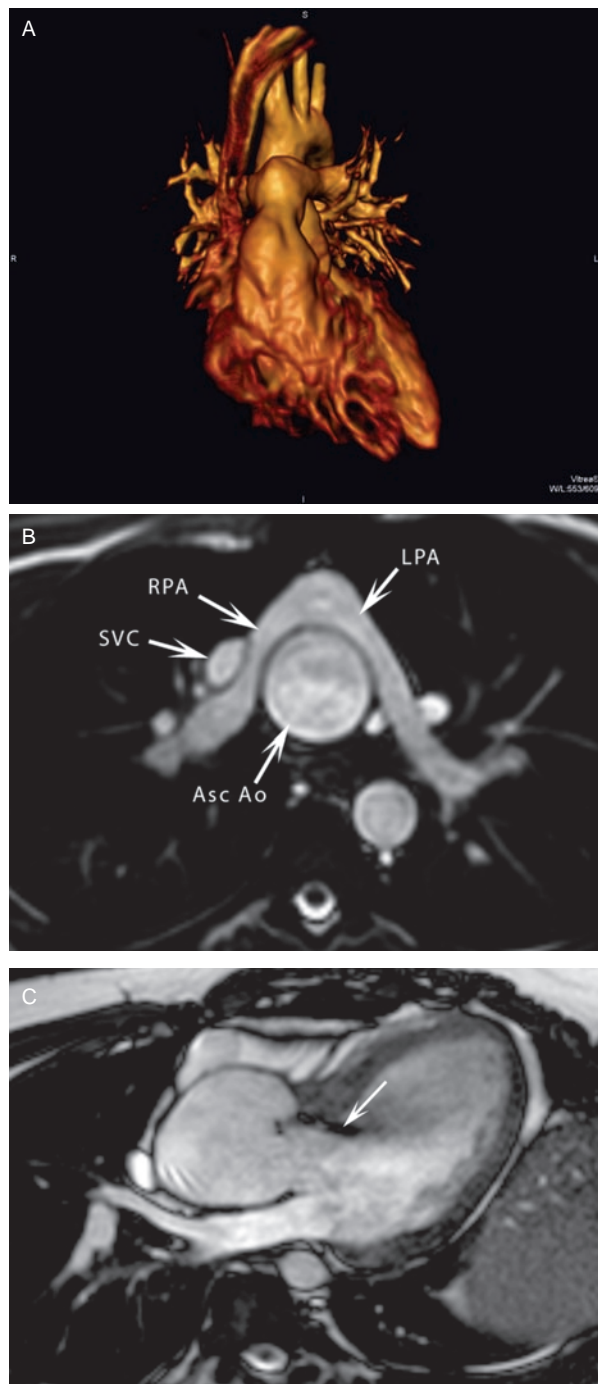
Figure 7 D-TGA. Post arterial switch. (A) Volume rendered image from a gadolinium enhanced MRA. Note the position of the pulmonary artery anterior to the aorta. (B) Axial image from a gadolinium enhanced MRA showing the location of the pulmonary arteries in front of the aorta. Note the mild stenosis of the right pulmonary artery (RPA) as it passes between the aorta and the SVC. D-TGA. (C) Left ventricular outflow tract (3-chamber) view in diastole showing a dilated aortic root with aortic regurgitation (arrow).

Table 1 Suggested MRI protocol for congenital heart disease

Scouts and reference scans (parallel imaging)

Interactive imaging for acquisition of scan plane geometries (four-chamber, short-axis, RVOT, LVOT, pulmonary trunk
through-plane, aorta through-plane, aortic arch, branch pulmonary arteries 2 orthogonal in-plane views and through-plane)

2D multi-slice b-SSFP cine images
    Whole ventricle in short-axis plane
    Alternatively, in complex conditions, to cover the whole heart in a transverse plane

2D single-slice b-SSFP cine images
    Four-chamber view
    RVOT (1–2 planes)
    LVOT (1–2 planes)
    Branch pulmonary arteries
    Aortic arch
    Targeted slices to address vascular stenoses

Phase-contrast velocity mapping
    Main pulmonary artery through-plane
    Ascending aorta through-plane
    Vascular stenosis in-plane or through-plane

2D multi-slice black-blood imaging (if previous scanning was unsatisfactory)
    Branch pulmonary arteries
    Aortic arch
    Vascular stenosis

3D contrast-enhanced MR angiography of the thoracic great vessels (1–3 dynamics)

Balanced-SSFP 3D 'whole-heart' volume scan (or if not available: conventional axial black-blood imaging)

LVOT, left ventricular outflow tract; RVOT, right ventricular outflow tract; SSFP, steady state free precession.
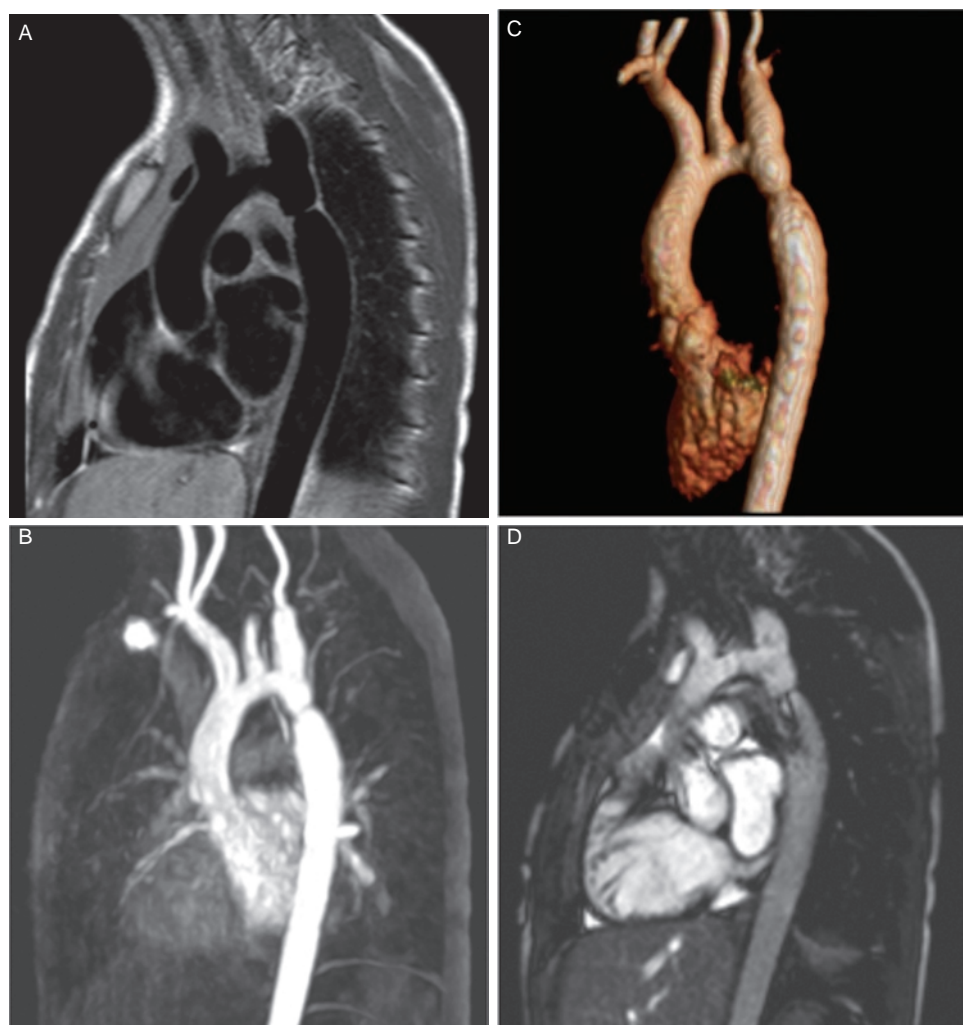
Figure 8 Circumscribed coarctation of the aorta. (A) Oblique sagittal black blood image showing a focal narrowing of the aorta just beyond the left subclavian artery. (B) Maximum intensity projection from a 3d Gadolinium enhanced MRA showing the coarctation. (C) Coarctation shown on a 3D volume rendered reconstruction from the Gadolinium enhanced MRA. (D) 2D SSFP image in oblique sagittal plane shows the coarctation and a dephasing jet (black) at the site of flow acceleration.

TOF including timing of pulmonary valve replacement.[31] [32] In patients with unrepaired TOF and pulmonary atresia cardiac MRI can define all the sources of arterial blood supply to the lungs including the presence, size and course of major aortopulmonary collaterals (figure 5), a patent ductus arteriosus and the anatomy of the central pulmonary arteries. 3D CE-MRA is a particularly useful technique in this regard.[33]

Complete transposition of the great arteries
Complete transposition of the great arteries, in which the aorta arises anterior and rightward from the right ventricle and the pulmonary artery arises posterior and leftward from the left ventricle is the most common form of transposition and is a common form of cyanotic CHD (accounting for 5–7% of patients born with CHD). Until the mid 1980s, this defect was surgically corrected with an atrial level switch (Senning or Mustard procedure). The arterial switch (Jatene procedure) became popular in the mid 1980s and is the current standard of care. In patients with the atrial switch procedure MRI provides information on quantitative right ventricular function, atrioventricular valve regurgitation, systemic venous or pulmonary venous pathway

obstruction and baffle leaks and stenosis[34] (figure 6). In patients postarterial switch procedure MRI is effective at detecting complications including right ventricular outflow tract and branch pulmonary artery obstruction, neo aortic root dilatation and coronary ostial occlusion[34–36] (figure 7).

Anomalies of the thoracic aorta
CMR is very effective for the evaluation of anomalies and diseases of the thoracic aorta. Although 2D echocardiography with Doppler is usually sufficient to diagnose and estimate the haemodynamic severity of coarctation of the aorta in infants, difficulties may be encountered in older children or adults. Under these circumstances the severity and extent of stenosis (figure 8), the collateral circulation well as the shape and size of the ascending aorta can be demonstrated by CMR.[37] [38] Velocity mapping can estimate the pressure gradient across the coarctation and the volume of collateral flow.[39] Thus, CMR is now regarded as the optimal modality for the evaluation of coarctation of the aorta including follow-up after surgery or angioplasty and also allows to assess LV function and mass accurately. CMR is also useful for the evaluation of sinus of Valsalva aneurysm, aortic dilatation,
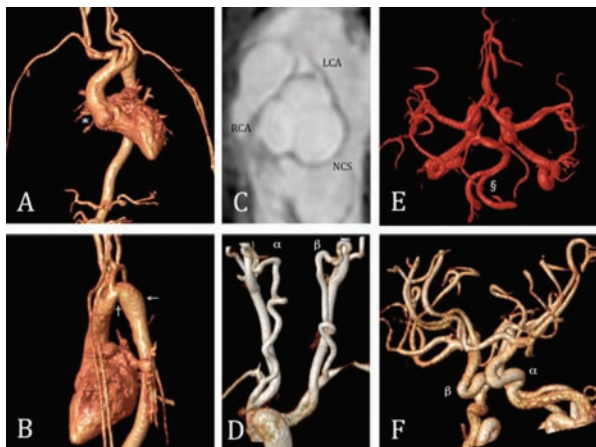
Figure 9 Loeys- Dietz Syndrome (A) 3D-shaded reconstruction from a 3D Gadolinium enhanced MAR anterior view. Dilated aortic root (*), ascending aorta (20x21mm, >P95), elongation of the whole thoracic aorta with marked kinking and tortuous course particularly of the transverse aortic arch. Left aortic arch. No aneurysm in the abdominal aorta. (B) Aortic arch kinking and narrowing (10x12mm) in the isthmic region (†). Mild dilatation of the upper descending aorta (¬) (16x15mm, >P95) and normal descending aorta. (C) 3D-SSFP reformatted plane through the dilated aortic sinus (32x34mm, >P95) at the level of the right (RCA) and left (LCA) coronary arteries offspring. Dilated and asymmetric non-coronary sinus (NCS). (D) 3D-shaded reconstruction from a 3D contrast enhanced MRA posterior view of supra aortic vessels. Tortuous left (a) and right (b) internal carotid arteries, with no discrete narrowing. (E) Shaded surface reconstruction from a 3D contrast enhanced MRA of the arterial circle of Willis, superior view. Marked tortuosity of all intracranial brain arteries and also of the extracranial basilaris/vertebral system (§), but no evidence for stenosis or aneurysm. (F) Shaded surface reconstruction from a 3D contrast enhanced MRA of the arterial circle of Willis, left anterior view. Tortuousity of the left (a) and right (b) internal carotid arteries.

aneurysm associated with Marfan and Ehler–Danlos syndromes, and in the general monitoring of aortic dimensions over time, such as with arterial tortuosity[40] ('Loeys–Dietz syndrome', figure 9). CMR is the procedure of choice for the diagnosis of aortic arch anomalies including vascular rings[25] (figures 10 and 11). Multidetector CT (MDCT) is an alternative imaging modality for the evaluation of anomalies of the thoracic aorta in children. It has the advantages of being widely available and ability to rapidly image the thoracic vasculature with high spatial resolution providing isotropic data sets.[41] However, the major drawback of MDCT is the need for ionising radiation.

'Pretricuspid' left-to-right shunts
CMR is helpful in selected patients with known or suspected atrial septal defects (ASDs), usually adolescents or adults with inconclusive clinical or echocardiographic findings.[42 43] It provides a non-invasive alternative to diagnostic catheterisation in patients with right ventricular volume overload in whom transthoracic echo cannot demonstrate the source of the left-to-right shunt such as in cases of sinus venous type ASDs (figure 12) and anomalous pulmonary venous connections. ASD location, size, relation to key neighbouring structures, its suitability for transcatheter versus surgical closure and functional assessment of haemodynamic burden including pulmonary to systemic flow ratio and right ventricular size and function can be accurately demonstrated by CMR. CMR is highly accurate for the diagnosis of anomalous


Figure 10 Double aortic arch. Volume rendered reconstruction from a 3D gadolinium enhanced MRA. The left arch is smaller and has a focal point of atresia (arrow).

venous pulmonary connections, allowing excellent visualisation of the entire course of all pulmonary veins within the mediastinum and lungs[44 45] (figure 13).

Single ventricle defects
Echocardiography is usually employed for the initial diagnosis and surgical planning of functional single ventricle defects such as the hypoplastic left heart syndrome and tricuspid atresia. CMR is occasionally used to supplement this information and is superior to echocardiography for quantifying ventricular volumes in these abnormalities. This information may be critical for surgical decisions regarding biventricular repair versus univentricular palliation[46] by means of the staged Norwood procedure resulting in a Fontan-type circulation (total cavopulmonary connection). CMR can be used to define ventricular and valvular function and vascular anatomy (figures 14 and 15) in infants with functional single ventricles during staged conversion to the Fontan circulation, obviating the need for invasive catheterisation in selected cases.[47] In a completed Fontan reconstruction of a single ventricle defect the use of CMR provides an excellent comprehensive assessment of anatomy, physiology and function to aid in further medical/surgical management.[48] An important structure to evaluate is the entire
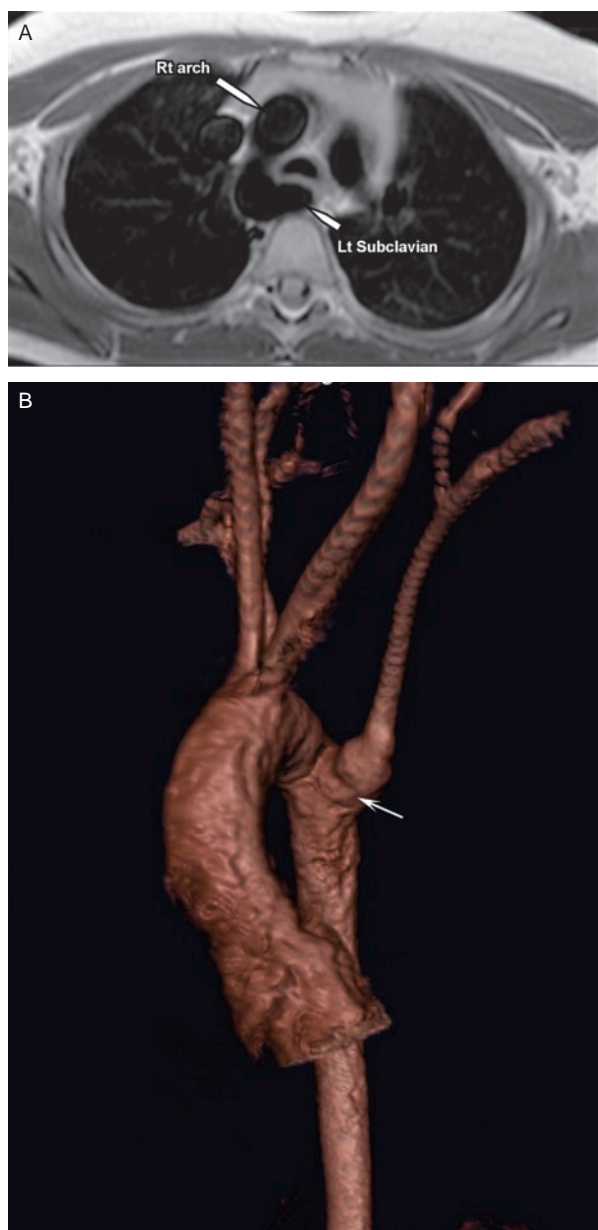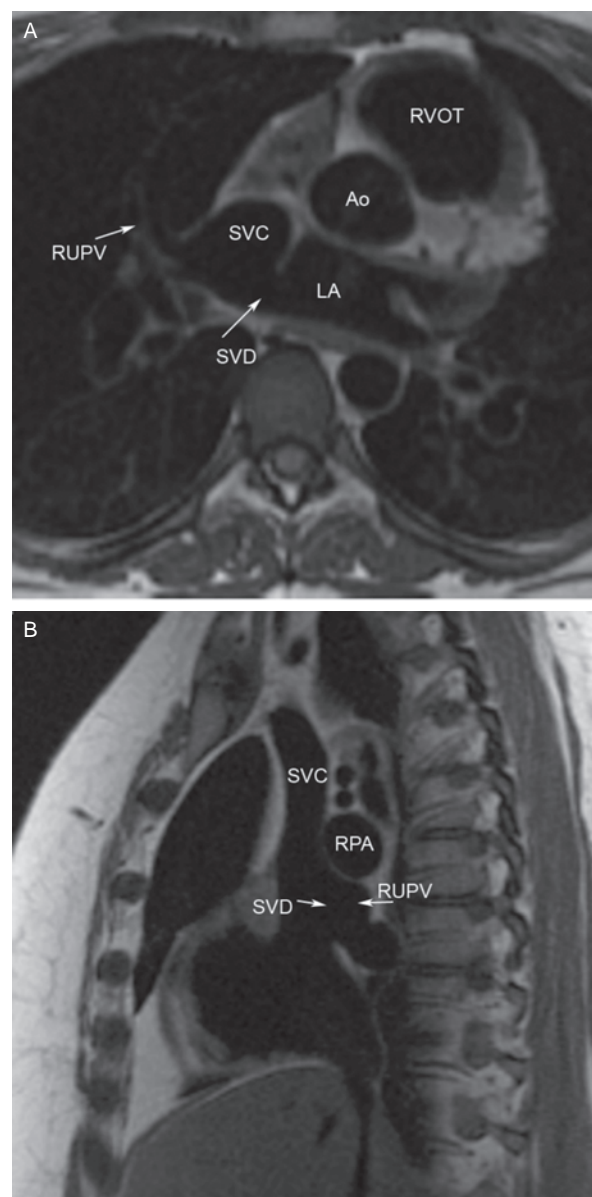
Figure 11 Right aortic arch with an aberrant subclavian artery. (A) Axial black blood image. (B) Volume rendered image from a 3D gadolinium enhanced MRA. Note the dilatation at the origin of the left subclavian artery (diverticulum of Komerrell, arrow), which indicates the presence and attachment of the ductus ligament.

Figure 12 Sinus venosus defect. (A) Axial and (B) sagittal oblique black blood images. The sinus venosus defect (SVD) is located between the posterior wall of the SVC and the anterior wall of the right upper lobe pulmonary vein (RUPV).

systemic venous pathway for obstructions (figure 16) or clot. Function of the single ventricle can be accurately assessed. Gadolinium-enhanced MRA is particularly helpful to determine the presence of collaterals (figure 17) and to evaluate the aortic arch.

Coronary artery anomalies

Congenital abnormalities in the course of the proximal coronary arteries can be reliably depicted by CMR both in patients with CHD and those with otherwise normal cardiac anatomy.[13 49] CMR has advantages over x-ray angiography in clarifying the spatial relationship of these arteries with respect to the aorta and the pulmonary artery, which is crucial for estimating the risk associated with these abnormalities and for surgical planning.

CMR has shown to be reliable and equivalent to x-ray angiography for the identification of coronary artery aneurysms in patients with Kawasaki disease (figure 18).[50 51] In addition CMR allows identification of perfusion defects, infarcts and abnormalities in ventricular function providing comprehensive assessment of cardiac involvement in Kawasaki disease.[52]

CLINICAL APPLICATIONS: CARDIAC TUMOURS

Transthoracic echocardiography is the usual technique which detects intracardiac tumours. However, in many cases evaluation is incomplete, and CMR is particularly helpful in determining the relationship to normal intracardiac structures, tumour extension to adjacent vascular and mediastinal structures and infiltration into the pericardium to aid in surgical planning. In addition signal intensity of the lesion
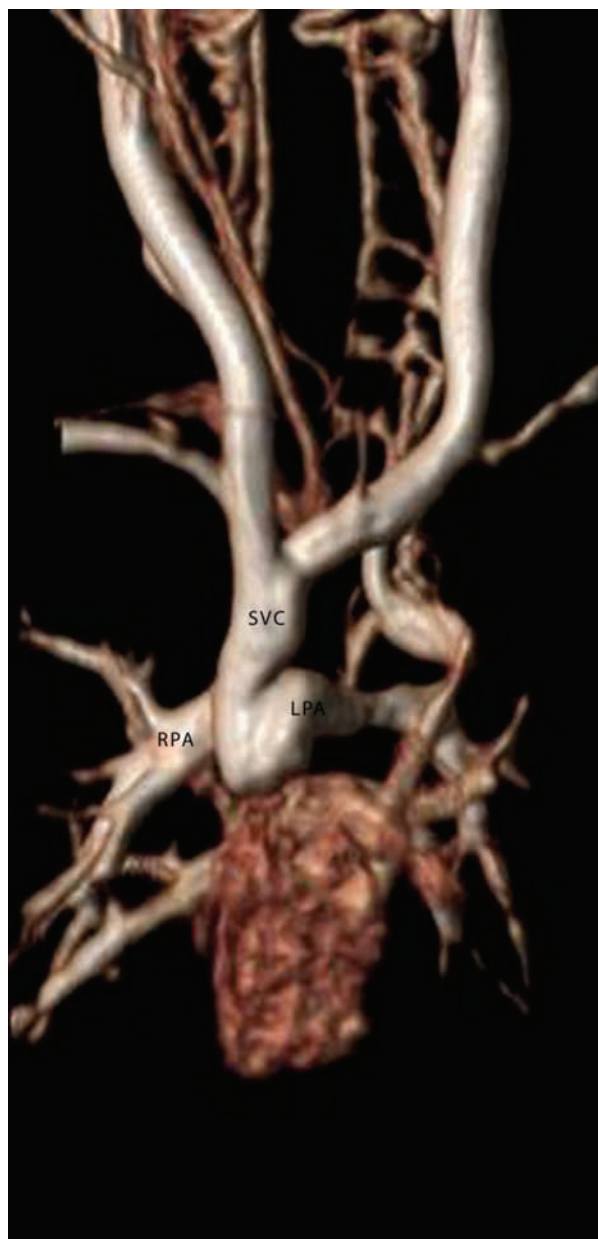
Review

Figure 13 Partial anomalous pulmonary venous return of the entire right lung to the SVC. 3D volume rendered image from a gadolinium enhanced MRA viewed from the posterior aspect. 3 pulmonary veins from the right lung (arrows) are seen entering the SVC.

on different MR sequences can assist in tumour characterisation. MR sequences for tissue characterisation include T1- and T2-weighted sequences, fat-suppressed sequences and postcontrast-enhanced sequences (figure 15). The signal intensity of a lesion is dependent on the interaction of the tissue composition and the CMR parameters employed for imaging. The differential diagnosis of a high signal intensity lesion on T1-weighted images includes fatty tumours (lipoma, liposarcoma), recent haemorrhage (due to methaemoglobin breakdown products), some cystic lesions (in case of a high protein content cyst) and melanoma (due to the effects of melanin). A lesion with low signal intensity on T1-weighted images may represent a cyst filled with low protein fluid, a signal void in a vascular malformation, a calcified lesion or the presence of air. High signal on T2-weighted imaging is typically produced by fluid-containing lesions such as cysts and inflammatory tissue. Fat-suppression techniques can be used to diagnose fatty content definitively. Further differentiation of the tumour can be made with the intravenous MR contrast agent gadolinium. During the first pass, vascular tumours (haemangioma, angiosarcoma) show early enhancement and small vessels may be easily identifiable. In the early phase, after injection at 1–2 min, necrotic areas in malignant tumours show as dark areas surrounded by enhancement elsewhere. In the later phase, malignant tumours typically show contrast enhancement indicating tissue vascularity. Such enhancement is usually absent in cystic lesions, and
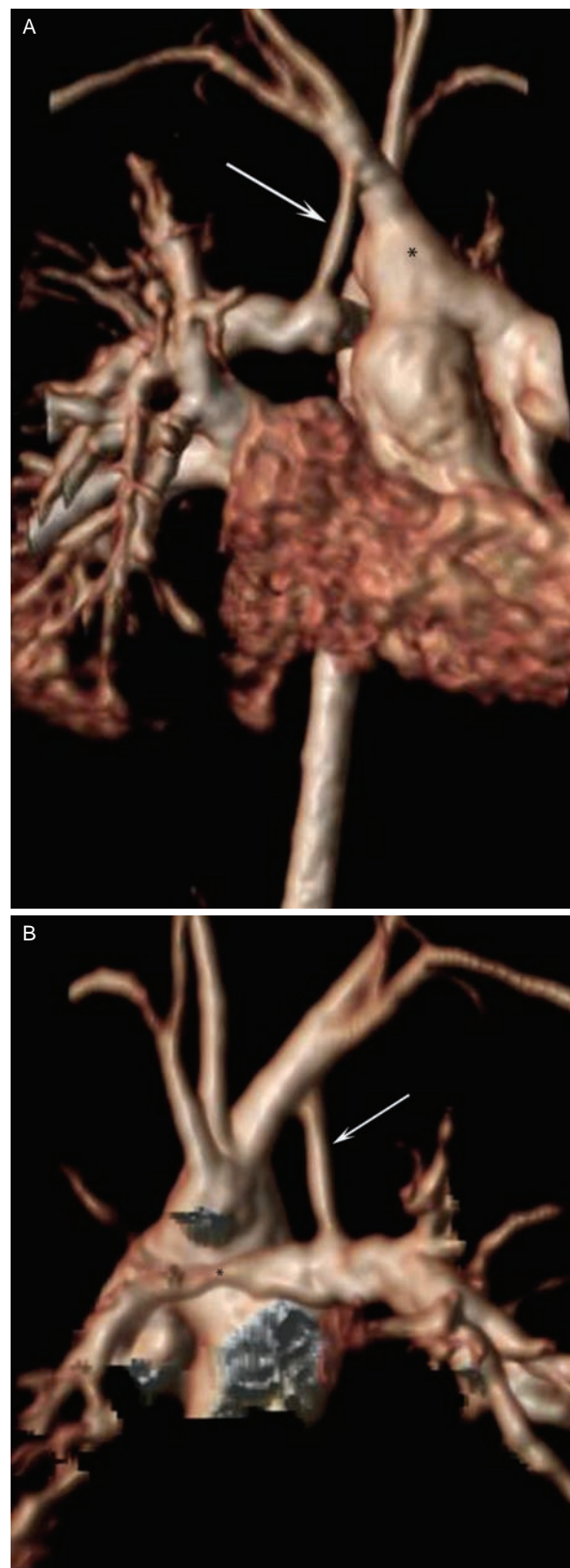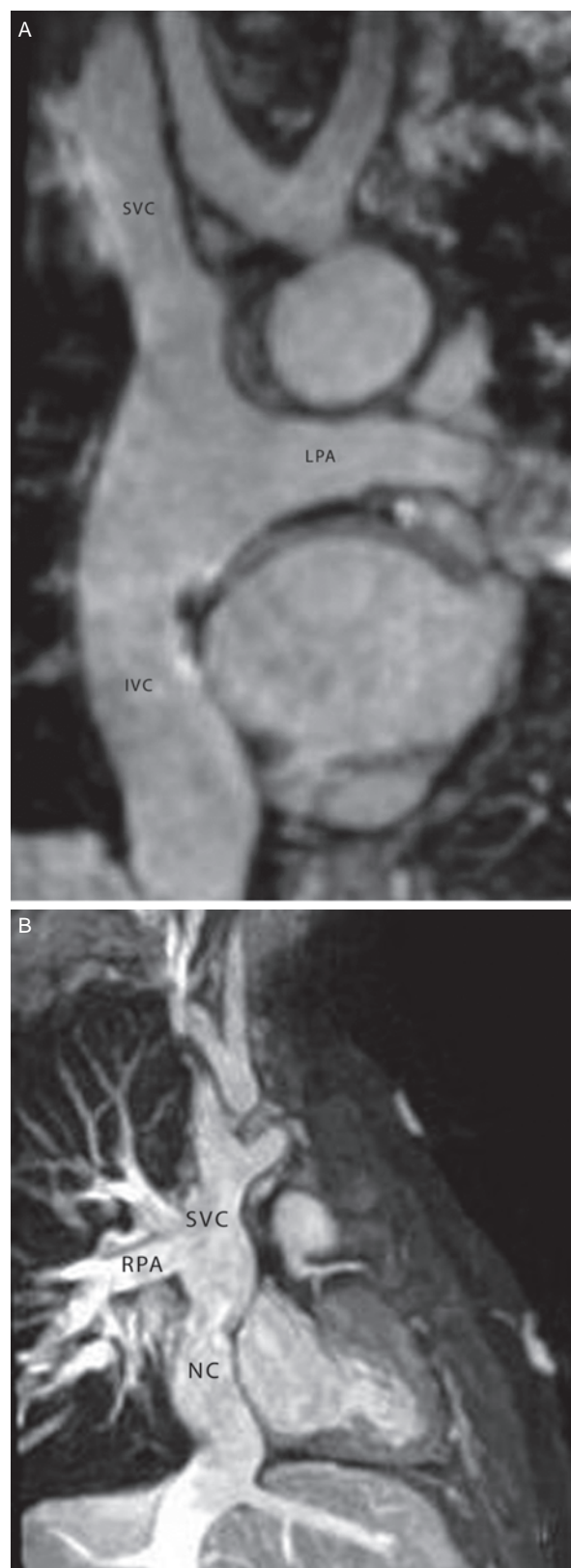

Figure 14 Post stage 1 Norwood palliation for HLHS. 3D volume rendered images from a gadolinium enhanced MRA. (A) View from the front showing the BT shunt (arrow) and the aorto pulmonary anastomosis (asterix). (B) View from the back showing the BT shunt (arrow) and a stenotic LPA (asterix).

Figure 15 HLHS Post Norwood 2. Hemifontan connection between the SVC and the RPA.

Figure 16 Lateral tunnel Fontan for HLHS in a 9-year-old with low oxygen saturations. Reconstructions from a sagittal 3D SSFP acquisition showing the patent connections of the IVC and the SVC to the LPA (Figure 13 A) and RPA (Figure 13B) junction.

most benign tumours (haemangiomas and myxomas being exceptions). Thrombus in the ventricles is shown by modern CMR sequences, particularly late gadolinium enhancement[53] and for this application MR may be more sensitive than echocardiography.

The most common primary heart tumours that occur in the paediatric age group are cardiac rhabdomyomas and cardiac fibromas.[54] Primary malignant tumours are extremely rare. Cardiac rhabdomyomas can arise in the setting of tuberous sclerosis (approximately 50%) or de novo, and they may be either multiple or solitary. They are the most common cardiac masses observed in children, are most frequently diagnosed at less than 1 year of age and may regress spontaneously. Cardiac fibromas are the second most common

Figure 17 Post Total Cavo Pulmonary Connection. 3D Gd MRA for laevoatrial cardial vein (horizontal arrow) reopening to form a massive innominate (vertical arrow) to left lower lobe pulmonary vein (asterix) collateral with significant right to left shunting and severe cyanosis.

cardiac mass diagnosed in childhood. Almost all cardiac fibromas arise from the left ventricle. Rhabdomyomas may appear isotense or mildly hyperintense to normal myocardium on T1- and T2-weighted images.[55] Fibromas often demonstrate T2-weighted signal hypointensity due to the fibrous nature of the mass; however, they may also be isointense to normal myocardium (figure 19).[55] Rhabdomyomas avidly enhance, often in a homogeneous fashion, and both early and delayed phase signal hyperintensity may be observed following the intravenous administration of gadolinium-containing contrast material. Fibromas show variable contrast enhancement.

CLINICAL APPLICATIONS: CARDIOMYOPATHIES
The cardiomyopathies include a variety of diseases where the primary pathology directly involves the myocardium excluding coronary artery disease. CMR is proving increasingly valuable in the identification and management of these conditions.

Hypertrophic cardiomyopathy (HCM) accounts for 42% of childhood cardiomyopathies and has an incidence of 0.47/100 000 children.[56] 2D and Doppler echocardiography are the most commonly used non-invasive methods to study HCM. However, the 3D nature of CMR allows for the precise definition of the site and the extent of hypertrophy, especially at the LV apex and anterolateral free wall which may not be well assessed by echocardiography. Especially in patients in whom echocardiography is technically unsatisfactory, CMR should be considered the technique of choice for diagnosing and following patients with all variants of HCM.[25] Late-enhancement gadolinium CMR has also been used in HCM to demonstrate areas of fibrosis, and the extent of this abnormal uptake is linked to the risk of sudden death and development of LV dilation and heart failure (figure 20).[57]

Left ventricular non-compaction (LVNC) is a rare congenital cardiomyopathy characterised by a thickened left ventricular myocardium with excessive trabeculation, and deep intertrabecular recesses communicating with the ventricular cavity.[58] LVNC may occur in association with other congenital heart defects, including atrial and ventricular septal defects, Ebsteins anomaly, congenital aortic stenosis and aortic coarctation. When no other congenital heart lesion is present, LVNC is said to be isolated. The clinical presentation varies considerably, with some patients showing no clinical symptoms and others presenting with severe heart failure or arrhythmias. In comparison to echocardiography MRI provides better delineation of the extent of the abnormal trabeculation in patients with non-compaction of the left ventricular myocardium (figure 21).[59] It is particularly useful when the myocardial involvement is subtle, as in asymptomatic family members. LVNC is diagnosed accurately with cardiac MR using a non-compacted to compacted myocardium ratio of ≥ 2.3 in diastole.[60]

CMR is a first-line imaging technique for investigating arrhythmogenic right ventricular cardiomyopathy (ARVC) and following progression in right ventricular volumes, structure and function over time. The diagnosis of ARVC is based on the presence of major and minor criteria encompassing genetic, electrocardiographic, arrhythmic, morphofunctional and histopathologic factors.[61] Specifically the diagnostic criteria of ARVC, which CMR can contribute to include, regional wall motion abnormalities of the right ventricle, increased right ventricular volumes with quantification, morphological abnormalities (aneurysms, trabecular disarray) and increased myocardial signal in the right ventricular wall suggesting fatty infiltration.[62] Focal wall motion abnormalities, especially focal dyskinesia, are generally felt to be a more reliable indicator of ARVC than intramyocardial fat.[63] More recently, late-gadolinium enhancement has been recognised as another interesting marker for ARVC.[64 65]

Iron overload cardiomyopathy due to excess iron deposition is associated with hereditary haemochromatosis and also a consequence of chronic transfusion therapy in a number of disorders including thalassemia, sickle cell anaemia, red cell aplasia and chronic renal failure. Heart failure due to myocardial iron overload remains the leading cause of death in patients with transfusion-dependent anaemias. The availability of a non-invasive technique to quantify myocardial iron is important because there is no significant relationship between the myocardial iron concentration and the different iron store parameters, nor with the liver iron concentrations. Iron overload-induced cardiomyopathy is reversible if intensive chelation therapy is instituted on time. Thus, early detection of myocardial iron deposition is imperative to prevent overt heart failure. Recently, measurement of an MR relaxation parameter T2-star (T2*) has been shown to reflect myocardial tissue iron, and there is a clear relation between reduced myocardial T2* (<20 ms) indicating iron overload, and LV dysfunction.[66] Myocardial T2* increases in concert with LV function recovery in thalassemia patients with heart failure. CMR has been used to evaluate different chelation regimes specifically for their action on the myocardium. Recently improved survival in thalassemia major has been attributed to the use of T2* CMR for assessing cardiac iron loading, thereby identifying patients at highest risk who require intensified iron chelation treatment.[67]

PERICARDIAL DISEASE
CMR is well suited to define anatomic abnormalities of the pericardium including pericardial thickening and effusions. In
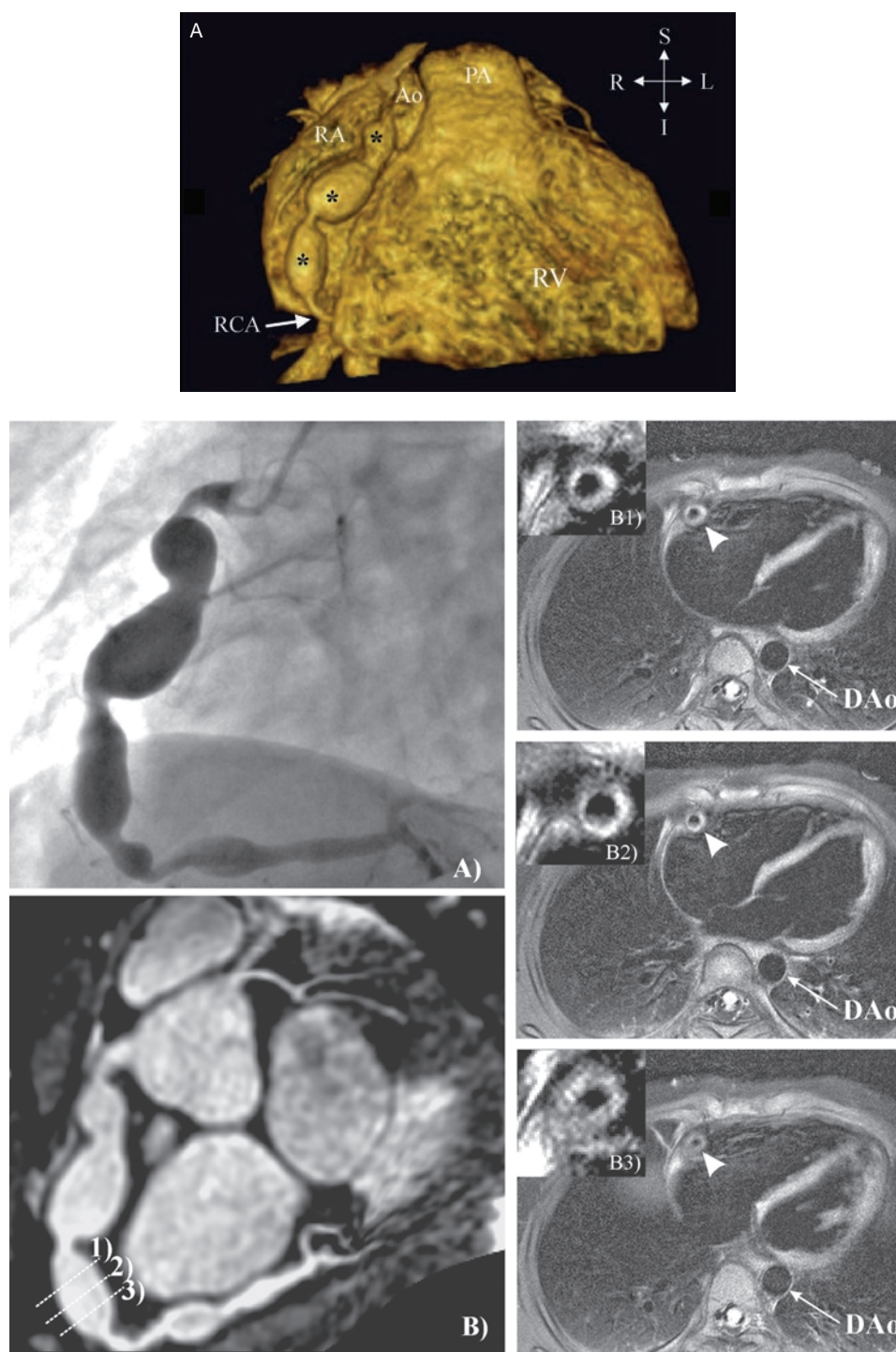
Figure 18 Coronary artery aneurysms in Kawasaki disease as shown by MRI. (A) Volume-rendered 3-D reconstruction (isotropic, whole-heart, 3D SSFP dataset) of the RCA with coronary artery aneurysms (asterisks) in a 7.8-year-old boy. (Ao, aorta; PA, pulmonary artery; RA, right atrium; RCA, right coronary artery; RV, right ventricle; S, superior; I, inferior; R, right; L, left). (B) Good agreement between the lateral X-ray angiogram (a) and the corresponding CMR image (b) for detection of the right coronary artery aneurysms. MR images were acquired with a whole-heart, 3D SSFP technique without the use of contrast agents. Sequential cross-sectional views of the aneurysm demonstrate a thickened vessel wall (arrowheads) at three different locations (B1, B2 and B3). Images were acquired with a 2- D black-blood spin-echo technique. In contrast to the right coronary artery aneurysms (B1, B2 and B3), the wall of the aorta (DAo) is normal.

addition CMR is able to depict and quantify the functional abnormalities which may be associated with pericardial disease. The large field of view of CMR is helpful in providing a better overview of the extent of pericardial disease, and to define the relationship with surrounding anatomic structure. In comparison to echocardiography CMR may be of diagnostic value in patients with loculated or complex configurations of pericardial effusions.

The characteristic anatomic and functional changes associated with constrictive pericardial disease (elongated and narrow RV, abnormal motion of the sigmoid-shaped interventricular septum, enlargement of the right atrium and inferior
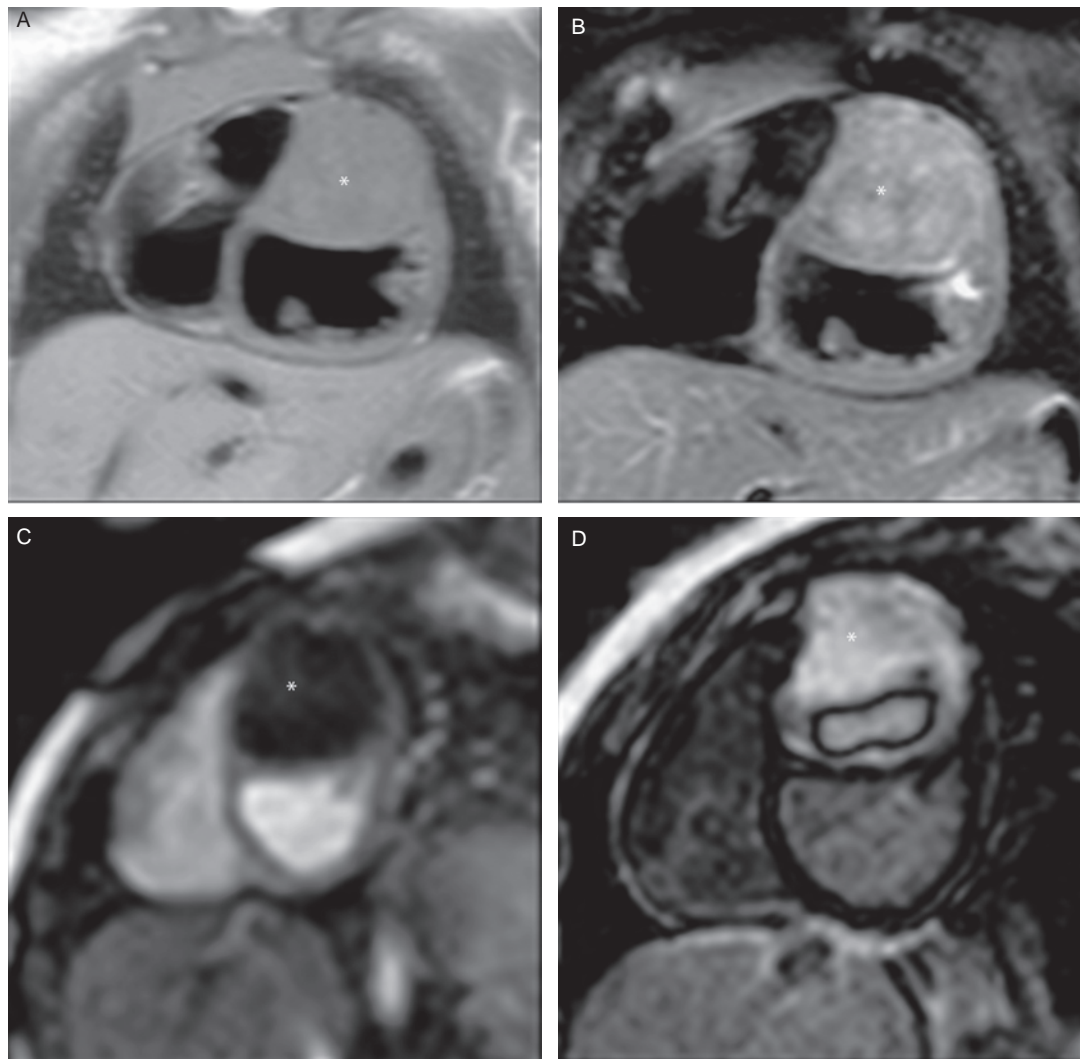
Figure 19 Cardiac Fibroma. Short axis views using a T1 (A) and T2 (B) weighted sequence shows the mass is of similar signal intensity to muscle. (C) The mass does not exhibit significant enhancement on 1st pass perfusion imaging. (D) Delayed enhancement shows enhancement of the majority of the mass except a ring of tissue in the core.

caval vein, stagnant blood in the atria and pericardial thickening) are clearly identified with CMR. Real-time MRI can demonstrate characteristic changes of the septal configuration during respiration indicating the haemodynamic severity of a given pericardial effusion.

Pericardial thickening is the hallmark of pericardial constriction (figure 22). CMR is superior to echocardiography in measuring pericardial thickness. The normal pericardium is <2 mm thick. A pericardial thickness of >4 mm has shown to be useful in identifying patients with constrictive pericarditis and differentiation from restrictive cardiomyopathy.[68] The finding of a diastolic septal bounce on cine MR is indicative of ventricular interdependence, a sign of constrictive physiology.[69] This can also be easily demonstrated by real-time MRI (see above).

FUTURE DEVELOPMENTS

Interventional MR is a new and highly promising tool that is under investigation at several centres and may soon find its way to routine clinical use. Cardiac catheterisation guided by MRI has been shown to be safe and practical in a clinical

setting. It allows better soft tissue visualisation, provides more pertinent physiological information and results in lower radiation exposure than do fluoroscopically guided procedures alone. Reported MR-guided catheter applications in humans include assessment of pulmonary vascular resistance and radiofrequency ablation procedures.[70] A range of other applications have been reported in animal models including ASD closure, aortic valve placements and stenting of aortic coarctation.[71]

In preliminary studies the application of novel intravascular blood pool contrast agents such as Vasovist (gadofosveset trisodium) has been shown to provide improved quality of cardiac imaging including better depiction of the coronary arterial and venous systems.[72 73]

Newer velocity-encoded MR sequences allowing resolution of velocity vectors in three directions, with spatial coverage of a 3D volume, temporally resolved throughout the cardiac cycle (7D flow encoding) are under development.[12 74]

High field strength magnets (3T) with multiple channels and faster gradients are under investigation and in future may allow rapid high-resolution imaging also in neonates and infants.
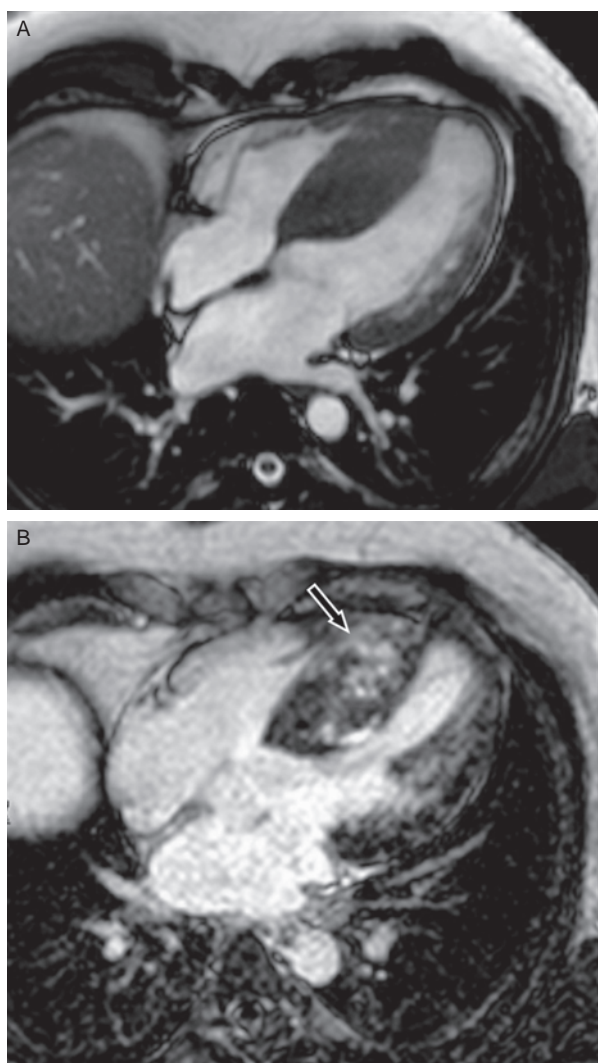
Figure 20 Hypertrophic cardiomyopathy (HCM). (A) Horizontal long axis (4-chamber) view showing the marked asymmetrical thickening of the septum. (B) Delayed enhancement image showing patchy enhancement of the hypertrophied septum (arrow).

SUMMARY

CMR offers several advantages over other imaging modalities, including superior soft tissue contrast, lack of ionising radiation, a capacity for true 3D imaging, accurate flow quantification and freely selectable imaging planes. These advantages and continued advances in MR hardware, software and imaging techniques are bringing CMR into more widespread use in paediatric cardiology. In routine clinical practice CMR is the technique of choice for postoperative assessment and follow-up of patients with CHD. Moreover, it allows tissue characterisation and determination of the extent of cardiac masses and has the ability to detect and classify primary heart muscle disease in childhood. The information provided by CMR is useful for treatment planning and, in many cases, may obviate potentially harmful cardiac catheterisation. The use of MR for guiding catheterisation and interventions within the cardiovascular system is an emerging application likely to find its way to clinical use in the near future.

Competing interests None.

Provenance and peer review Commissioned; externally peer reviewed.
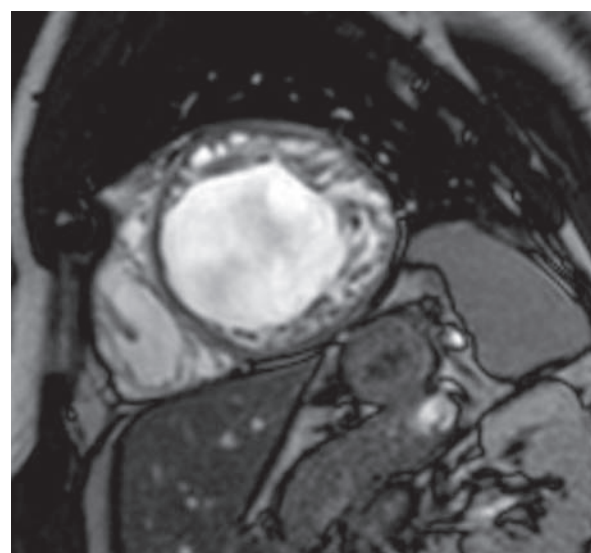
Figure 21 Left ventricular non compaction. Short axis view using a cine bright blood image showing the hypertrabeculated left ventricular myocardium with deep recesses communicating with the ventricular cavity.
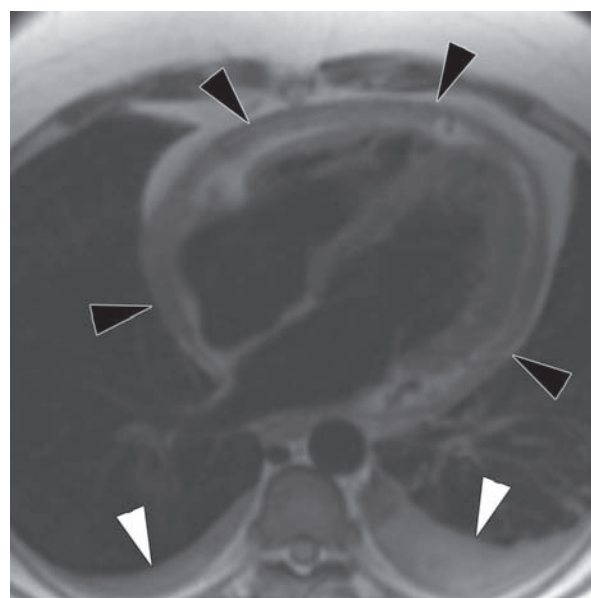
Figure 22 Constrictive pericarditis. Axial black blood imaging showing the marked pericardial thickening (black arrow heads) and bilateral pleural effusions (white arrow heads).

REFERENCES

1. **Mulkern RV,** Chung T. From signal to image: magnetic resonance imaging physics for cardiac magnetic resonance. *Pediatr Cardiol* 2000;**21**:5–17.
2. **Simonetti OP,** Cook S. Technical aspects of pediatric CMR. *J Cardiovasc Magn Reson* 2006;**8**:581–93.
3. **Chia JM,** Fischer SE, Wickline SA, *et al.* Performance of QRS detection for cardiac magnetic resonance imaging with a novel vectorcardiographic triggering method. *J Magn Reson Imaging* 2000;**12**:678–88.
4. **Körperich H,** Gieseke J, Barth P, *et al.* Flow volume and shunt quantification in pediatric congenital heart disease by real-time magnetic resonance velocity mapping: a validation study. *Circulation* 2004;**109**:1987–93.
5. **Kaji S,** Yang PC, Kerr AB, *et al.* Rapid evaluation of left ventricular volume and mass without breath-holding using real-time interactive cardiac magnetic resonance imaging system. *J Am Coll Cardiol* 2001;**38**:527–33.
6. **Simonetti OP,** Finn JP, White RD, *et al.* "Black blood" T2-weighted inversion-recovery MR imaging of the heart. *Radiology* 1996;**199**:49–57.

Review

7. **Carr JC,** Simonetti O, Bundy J, *et al.* Cine MR angiography of the heart with segmented true fast imaging with steady-state precession. *Radiology* 2001;**219**:828–34.

8. **Plein S,** Bloomer TN, Ridgway JP, *et al.* Steady-state free precession magnetic resonance imaging of the heart: comparison with segmented k-space gradient-echo imaging. *J Magn Reson Imaging* 2001;**14**:230–6.

9. **Bellenger NG,** Burgess MI, Ray SG, *et al.* Comparison of left ventricular ejection fraction and volumes in heart failure by echocardiography, radionuclide ventriculography and cardiovascular magnetic resonance; are they interchangeable? *Eur Heart J* 2000;**21**:1387–96.

10. **Bellenger NG,** Davies LC, Francis JM, *et al.* Reduction in sample size for studies of remodeling in heart failure by the use of cardiovascular magnetic resonance. *J Cardiovasc Magn Reson* 2000;**2**:271–8.

11. **Grothues F,** Moon JC, Bellenger NG, *et al.* Interstudy reproducibility of right ventricular volumes, function, and mass with cardiovascular magnetic resonance. *Am Heart J* 2004;**147**:218–23.

12. **Sørensen TS,** Körperich H, Greil GF, *et al.* Operator-independent isotropic three-dimensional magnetic resonance imaging for morphology in congenital heart disease: a validation study. *Circulation* 2004;**110**:163–9.

13. **Beerbaum P,** Sarikouch S, Laser KT, *et al.* Coronary anomalies assessed by whole-heart isotropic 3D magnetic resonance imaging for cardiac morphology in congenital heart disease. *J Magn Reson Imaging* 2009;**29**:320–7.

14. **Beerbaum P,** Körperich H, Barth P, *et al.* Noninvasive quantification of left-to-right shunt in pediatric patients: phase-contrast cine magnetic resonance imaging compared with invasive oximetry. *Circulation* 2001;**103**:2476–82.

15. **Rebergen SA,** Chin JG, Ottenkamp J, *et al.* Pulmonary regurgitation in the late postoperative follow-up of tetralogy of Fallot. Volumetric quantitation by nuclear magnetic resonance velocity mapping. *Circulation* 1993;**88**:2257–66.

16. **Kilner PJ,** Firmin DN, Rees RS, *et al.* Valve and great vessel stenosis: assessment with MR jet velocity mapping. *Radiology* 1991;**178**:229–35.

17. **Powell AJ,** Tsai-Goodman B, Prakash A, *et al.* Comparison between phase-velocity cine magnetic resonance imaging and invasive oximetry for quantification of atrial shunts. *Am J Cardiol* 2003;**91**:1523–5, A9.

18. **Körperich H,** Gieseke J, Esdorn H, *et al.* Ultrafast time-resolved contrast-enhanced 3D pulmonary venous cardiovascular magnetic resonance angiography using SENSE combined with CENTRA-keyhole. *J Cardiovasc Magn Reson* 2007;**9**:77–87.

19. **Shellock FG,** Spinazzi A. MRI safety update 2008: part 2, screening patients for MRI. *AJR Am J Roentgenol* 2008;**191**:1140–9.

20. **Shellock FG,** Spinazzi A. MRI safety update 2008: part 1, MRI contrast agents and nephrogenic systemic fibrosis. *AJR Am J Roentgenol* 2008;**191**:1129–39.

21. **Shellock FG,** Crues JV. MR procedures: biologic effects, safety, and patient care. *Radiology* 2004;**232**:635–52.

22. **Shinbane JS,** Colletti PM, Shellock FG. MR in patients with pacemakers and ICDs: defining the issues. *J Cardiovasc Magn Reson* 2007;**9**:5–13.

23. **Sarikouch S,** Schaeffler R, Körperich H, *et al.* Cardiovascular magnetic resonance imaging for intensive care infants: safe and effective? *Pediatr Cardiol* 2009;**30**:146–52.

24. **Hendel RC,** Patel MR, Kramer CM, *et al.* ACCF/ACR/SCCT/SCMR/ASNC/ NASCI/SCAI/SIR 2006 appropriateness criteria for cardiac computed tomography and cardiac magnetic resonance imaging: a report of the American College of Cardiology Foundation Quality Strategic Directions Committee Appropriateness Criteria Working Group, American College of Radiology, Society of Cardiovascular Computed Tomography, Society for Cardiovascular Magnetic Resonance, American Society of Nuclear Cardiology, North American Society for Cardiac Imaging, Society for Cardiovascular Angiography and Interventions, and Society of Interventional Radiology. *J Am Coll Cardiol* 2006;**48**:1475–97.

25. **Pennell DJ,** Sechtem UP, Higgins CB, *et al.* Clinical indications for cardiovascular magnetic resonance (CMR): Consensus Panel report. *Eur Heart J* 2004;**25**:1940–65.

26. **Greil GF,** Beerbaum P, Razavi R, *et al.* Imaging the right ventricle: non-invasive imaging. *Heart* 2008;**94**:803–8.

27. **Mooij CF,** de Wit CJ, Graham DA, *et al.* Reproducibility of MRI measurements of right ventricular size and function in patients with normal and dilated ventricles. *J Magn Reson Imaging* 2008;**28**:67–73.

28. **Muthurangu V,** Razavi R, Bogaert J, *et al. Congenital heart disease.* In: Bogaert J, Dymarkowski S, Taylor AM., eds. *Clinical cardiac MRI with interactive CD-ROM.* Berlin, New York: Springer, 2005:549.

29. **Geva T,** Sandweiss BM, Gauvreau K, *et al.* Factors associated with impaired clinical status in long-term survivors of tetralogy of Fallot repair evaluated by magnetic resonance imaging. *J Am Coll Cardiol* 2004;**43**:1068–74.

30. **Knauth AL,** Gauvreau K, Powell AJ, *et al.* Ventricular size and function assessed by cardiac MRI predict major adverse clinical outcomes late after tetralogy of Fallot repair. *Heart* 2008;**94**:211–16.

31. **Frigiola A,** Tsang V, Bull C, *et al.* Biventricular response after pulmonary valve replacement for right ventricular outflow tract dysfunction: is age a predictor of outcome? *Circulation* 2008;**118**:S182–90.

32. **Oosterhof T,** van Straten A, Vliegen HW, *et al.* Preoperative thresholds for pulmonary valve replacement in patients with corrected tetralogy of Fallot using cardiovascular magnetic resonance. *Circulation* 2007;**116**:545–51.

33. **Geva T,** Greil GF, Marshall AC, *et al.* Gadolinium-enhanced 3-dimensional magnetic resonance angiography of pulmonary blood supply in patients with complex pulmonary stenosis or atresia: comparison with x-ray angiography. *Circulation* 2002;**106**:473–8.

34. **Dorfman AL,** Geva T. Magnetic resonance imaging evaluation of congenital heart disease: conotruncal anomalies. *J Cardiovasc Magn Reson* 2006;**8**:645–59.

35. **Gutberlet M,** Boeckel T, Hosten N, *et al.* Arterial switch procedure for D-transposition of the great arteries: quantitative midterm evaluation of hemodynamic changes with cine MR imaging and phase-shift velocity mapping-initial experience. *Radiology* 2000;**214**:467–75.

36. **Taylor AM,** Dymarkowski S, Hamaekers P, *et al.* MR coronary angiography and late-enhancement myocardial MR in children who underwent arterial switch surgery for transposition of great arteries. *Radiology* 2005;**234**:542–7.

37. **Nielsen JC,** Powell AJ, Gauvreau K, *et al.* Magnetic resonance imaging predictors of coarctation severity. *Circulation* 2005;**111**:622–8.

38. **Oshinski JN,** Parks WJ, Markou CP, *et al.* Improved measurement of pressure gradients in aortic coarctation by magnetic resonance imaging. *J Am Coll Cardiol* 1996;**28**:1818–26.

39. **Steffens JC,** Bourne MW, Sakuma H, *et al.* Quantification of collateral blood flow in coarctation of the aorta by velocity encoded cine magnetic resonance imaging. *Circulation* 1994;**90**:937–43.

40. **Valverde I,** Simpson J, Beerbaum P. Magnetic resonance imaging findings in Loeys-Dietz syndrome. *Cardiol Young* 2010;**20**:210–13.

41. **Dillman JR,** Hernandez RJ. Role of CT in the evaluation of congenital cardiovascular disease in children. *AJR Am J Roentgenol* 2009;**192**:1219–31.

42. **Beerbaum P,** Körperich H, Esdorn H, *et al.* Atrial septal defects in pediatric patients: noninvasive sizing with cardiovascular MR imaging. *Radiology* 2003;**228**:361–9.

43. **Beerbaum P,** Parish V, Bell A, *et al.* Atypical atrial septal defects in children: noninvasive evaluation by cardiac MRI. *Pediatr Radiol* 2008;**38**:1188–94.

44. **Greil GF,** Powell AJ, Gildein HP, *et al.* Gadolinium-enhanced three-dimensional magnetic resonance angiography of pulmonary and systemic venous anomalies. *J Am Coll Cardiol* 2002;**39**:335–41.

45. **Grosse-Wortmann L,** Al-Otay A, Goo HW, *et al.* Anatomical and functional evaluation of pulmonary veins in children by magnetic resonance imaging. *J Am Coll Cardiol* 2007;**49**:993–1002.

46. **Grosse-Wortmann L,** Yun TJ, Al-Radi O, *et al.* Borderline hypoplasia of the left ventricle in neonates: insights for decision-making from functional assessment with magnetic resonance imaging. *J Thorac Cardiovasc Surg* 2008;**136**:1429–36.

47. **Muthurangu V,** Taylor AM, Hegde SR, *et al.* Cardiac magnetic resonance imaging after stage I Norwood operation for hypoplastic left heart syndrome. *Circulation* 2005;**112**:3256–63.

48. **Fogel MA.** Cardiac magnetic resonance of single ventricles. *J Cardiovasc Magn Reson* 2006;**8**:661–70.

49. **Bunce NH,** Lorenz CH, Keegan J, *et al.* Coronary artery anomalies: assessment with free-breathing three-dimensional coronary MR angiography. *Radiology* 2003;**227**:201–8.

50. **Greil GF,** Stuber M, Botnar RM, *et al.* Coronary magnetic resonance angiography in adolescents and young adults with kawasaki disease. *Circulation* 2002;**105**:908–11.

51. **Mavrogeni S,** Papadopoulos G, Douskou M, *et al.* Magnetic resonance angiography is equivalent to X-ray coronary angiography for the evaluation of coronary arteries in Kawasaki disease. *J Am Coll Cardiol* 2004;**43**:649–52.

52. **Mavrogeni S,** Papadopoulos G, Douskou M, *et al.* Magnetic resonance angiography, function and viability evaluation in patients with Kawasaki disease. *J Cardiovasc Magn Reson* 2006;**8**:493–8.

53. **Weinsaft JW,** Kim HW, Shah DJ, *et al.* Detection of left ventricular thrombus by delayed-enhancement cardiovascular magnetic resonance prevalence and markers in patients with systolic dysfunction. *J Am Coll Cardiol* 2008;**52**:148–57.

54. **Becker AE.** Primary heart tumors in the pediatric age group: a review of salient pathologic features relevant for clinicians. *Pediatr Cardiol* 2000;**21**:317–23.

55. **Luna A,** Ribes R, Caro P, *et al.* Evaluation of cardiac tumors with magnetic resonance imaging. *Eur Radiol* 2005;**15**:1446–55.

56. **Lipshultz SE,** Sleeper LA, Towbin JA, *et al.* The incidence of pediatric cardiomyopathy in two regions of the United States. *N Engl J Med* 2003;**348**:1647–55.

57. **Moon JC,** McKenna WJ, McCrohon JA, *et al.* Toward clinical risk assessment in hypertrophic cardiomyopathy with gadolinium cardiovascular magnetic resonance. *J Am Coll Cardiol* 2003;**41**:1561–7.

58. **Weiford BC,** Subbarao VD, Mulhern KM. Noncompaction of the ventricular myocardium. *Circulation* 2004;**109**:2965–71.

59. **Alhabshan F,** Smallhorn JF, Golding F, *et al.* Extent of myocardial non-compaction: comparison between MRI and echocardiographic evaluation. *Pediatr Radiol* 2005;**35**:1147–51.

60. **Petersen SE,** Selvanayagam JB, Wiesmann F, *et al.* Left ventricular non-compaction: insights from cardiovascular magnetic resonance imaging. *J Am Coll Cardiol* 2005;**46**:101–5.

61. **McKenna WJ,** Thiene G, Nava A, *et al.* Diagnosis of arrhythmogenic right ventricular dysplasia/cardiomyopathy. Task Force of the Working Group Myocardial and Pericardial Disease of the European Society of Cardiology and of the Scientific Council on Cardiomyopathies of the International Society and Federation of Cardiology. *Br Heart J* 1994;**71**:215–18.

62. **Sen-Chowdhry S,** Prasad SK, Syrris P, *et al.* Cardiovascular magnetic resonance in arrhythmogenic right ventricular cardiomyopathy revisited: comparison with task force criteria and genotype. *J Am Coll Cardiol* 2006;**48**:2132–40.

63. **Tandri H,** Macedo R, Calkins H, *et al.* Role of magnetic resonance imaging in arrhythmogenic right ventricular dysplasia: insights from the North American arrhythmogenic right ventricular dysplasia (ARVD/C) study. *Am Heart J* 2008;**155**:147–53.

64. **Hunold P,** Wieneke H, Bruder O, *et al.* Late enhancement: a new feature in MRI of arrhythmogenic right ventricular cardiomyopathy? *J Cardiovasc Magn Reson* 2005;**7**:649–55.

65. **Tandri H,** Saranathan M, Rodriguez ER, *et al.* Noninvasive detection of myocardial fibrosis in arrhythmogenic right ventricular cardiomyopathy using delayed-enhancement magnetic resonance imaging. *J Am Coll Cardiol* 2005;**45**:98–103.

66. **Anderson LJ,** Holden S, Davis B, *et al.* Cardiovascular T2-star (T2*) magnetic resonance for the early diagnosis of myocardial iron overload. *Eur Heart J* 2001;**22**:2171–9.

67. **Modell B,** Khan M, Darlison M, *et al.* Improved survival of thalassaemia major in the UK and relation to T2* cardiovascular magnetic resonance. *J Cardiovasc Magn Reson* 2008;**10**:42.

68. **Masui T,** Finck S, Higgins CB. Constrictive pericarditis and restrictive cardiomyopathy: evaluation with MR imaging. *Radiology* 1992;**182**:369–73.

69. **Giorgi B,** Mollet NR, Dymarkowski S, *et al.* Clinically suspected constrictive pericarditis: MR imaging assessment of ventricular septal motion and configuration in patients and healthy subjects. *Radiology* 2003;**228**:417–24.

70. **Razavi R,** Hill DL, Keevil SF, *et al.* Cardiac catheterisation guided by MRI in children and adults with congenital heart disease. *Lancet* 2003;**362**:1877–82.

71. **Lederman RJ.** Cardiovascular interventional magnetic resonance imaging. *Circulation* 2005;**112**:3009–17.

72. **Chiribiri A,** Kelle S, Götze S, *et al.* Visualization of the cardiac venous system using cardiac magnetic resonance. *Am J Cardiol* 2008;**101**:407–12.

73. **Kelle S,** Thouet T, Tangcharoen T, *et al.* Whole-heart coronary magnetic resonance angiography with MS-325 (Gadofosveset). *Med Sci Monit* 2007;**13**:CR469–474.

74. **Markl M,** Chan FP, Alley MT, *et al.* Time-resolved three-dimensional phase-contrast MRI. *J Magn Reson Imaging* 2003;**17**:499–506.

Cardiovascular MRI in childhood

Anil K Attili, Victoria Parish, Israel Valverde, et al.

	Updated information and services can be found at:
	http://adc.bmj.com/content/early/2010/09/29/adc.2009.179051.full.html

These include:

References	This article cites 73 articles, 45 of which can be accessed free at: http://adc.bmj.com/content/early/2010/09/29/adc.2009.179051.full.html#ref-list-1
P<P	Published online September 29, 2010 in advance of the print journal.
Email alerting service	Receive free email alerts when new articles cite this article. Sign up in the box at the top right corner of the online article.

Notes

Advance online articles have been peer reviewed and accepted for publication but have not yet appeared in the paper journal (edited, typeset versions may be posted when available prior to final publication). Advance online articles are citable and establish publication priority; they are indexed by PubMed from initial publication. Citations to Advance online articles must include the digital object identifier (DOIs) and date of initial publication.